

Zhang, Y.P., Zhang, P.Z., Lease, R.O., Zhou, R., Wang, Y.J., Yan, Y.G., Wang, Y., Zheng, W.J., Liu, B.X., Li, Z.G., Liang, H., Hui, G.G., Sun, C., Tian, Q.Y., Xu, B.B., and Wang, W.T., 2023, Oligocene-Miocene Northward Growth of the Tibetan Plateau: Insights from Intermontane Basins in the West Qinling Belt, NW China: GSA Bulletin, <https://doi.org/10.1130/B36722.1>.

Supplemental Material

Text S1. Demagnetization and tests.

Text S2. Anisotropy of magnetic susceptibility (AMS) analyses.

Text S3. Detrital Zircons U-Pb Ages test.

Figure S1. Anhua sampling section.

Figure S2. Photographs of the sampled Anhua-Huicheng basin section.

Figure S3. Orthogonal (Zijderveld) vector plots of the representative thermal demagnetization behaviors of specimens from the Anhua section.

Figure S4. Equal-area plots of accepted ChRMs (185 sites) from the Anhua section in (a) geographic and (b) tilt-corrected coordinates.

Figure S5. AMS data. (a) Equal-area, lower-hemisphere projection of anisotropy of the maximum (blue squares), medium (green triangles) and minimum (pink circles) susceptibility axes in stratigraphic coordinates. (b) P_J-T (corrected degrees of anisotropy vs. shape parameter). (c) Flinn diagram.

Table S1. Main characteristics and interpretations of major sedimentary facies in this study.

Table S2. Fossils were discovered along the West Qinling Belt.

Table S3. Zircon U-Pb geochronological analyses.

Table S4. Quantitative comparison of age distributions for the Anhua basin (Z1&Z2; Z3&Z4).

1 Supplemental Material

2 **Text S1.** Demagnetization and tests.

3 **Text S2.** Anisotropy of magnetic susceptibility (AMS) analyses.

4 **Text S3.** Detrital Zircons U-Pb Ages test.

5 **Figure S1.** Anhua sampling section.

6 **Figure S2.** Photographs of the sampled Anhua-Huicheng basin section.

7 **Figure S3.** Orthogonal (Zijderveld) vector plots of the representative thermal demagnetization
8 behaviors of specimens from the Anhua section.

9 **Figure S4.** Equal-area plots of accepted ChRMs (185 sites) from the Anhua section in (a)
10 geographic and (b) tilt-corrected coordinates.

11 **Figure S5.** AMS data. (a) Equal-area, lower-hemisphere projection of anisotropy of the
12 maximum (blue squares), medium (green triangles) and minimum (pink circles) susceptibility
13 axes in stratigraphic coordinates. (b) P_J-T (corrected degrees of anisotropy vs. shape parameter).
14 (c) Flinn diagram.

15 **Table S1.** Main characteristics and interpretations of major sedimentary facies in this study.

16 **Table S2.** Fossils were discovered along the West Qinling Belt.

17 **Table S3.** Zircon U-Pb geochronological analyses.

18 **Table S4.** Quantitative comparison of age distributions for the Anhua basin (Z1&Z2; Z3&Z4).

19

20 **Text S1** Demagnetization and tests

21 The intensity of the natural remanent magnetization (NRM) for these specimens was 10^{-2} - 10^{-4} A/m.

22 Progressive thermal demagnetization successfully resolved multiple components of magnetization.

23 After the removal of only one or two secondary components of magnetization, the majority of

24 samples exhibit a linear decay to the origin (Figure S1). The low-temperature component was

25 typically removed at 200-250°C, but sometimes not until 450°C. We interpreted this low-

26 temperature component as the removal of secondary remanent magnetization. The high-temperature

27 component decays toward the origin, typically exhibits stable behavior between 450°C and 670°C,

28 and is interpreted to reflect the characteristic remanent magnetization (ChRM). Most samples show

29 an accelerated decay in remanent intensity just below 580°C or 680°C, indicating that magnetite

30 and hematite are the major magnetic carriers in these redness deposits (Figure 9). For most samples

31 throughout the stratigraphic section, there is no significant difference in remanence direction, when

32 it is defined by the 450-580°C or 600-670°C parts of the unblocking temperature spectra. This

33 suggests that both magnetic carriers recorded the same paleomagnetic field when their remanences

34 became fixed in the rock.

35 ChRM directions were determined by at least four, typically five to eight points from the stable

36 high-temperature component ($>450^\circ\text{C}$) in the demagnetization trajectory as implemented in Pmag

37 3.1 b2 (Jones, 2002). By principal component analysis, ChRM directions with maximum angular

38 deviation (MAD) above 15° were rejected from further analyses, thus discarding 17 (5%) of the

39 measured specimens. Virtual geomagnetic poles (VGPs) were then calculated based on the magnetic

40 declination and inclination. Samples with VGPs $< 10^\circ$ were not used to define the magnetic polarity

41 stratigraphy for the Anhua section. This eliminated 81 sampled horizons. Finally, a total of 185

42 (65%) samples were accepted to construct the magnetic polarity sequence of the Anhua section.
43 Of the 283 samples, 107 are of normal polarity and 75 are of reverse polarity. The mean directions
44 for normal and reversal polarity poles are $D_g = 33.8^\circ$, $I_g = 44.0^\circ$ with $k_g = 7.3$, $\alpha_{95} = 5.9$, and $D_s =$
45 191.8° , $I_g = 42.3^\circ$ with $k_g = 5.9$, $\alpha_{95} = 7.4$ in geographic coordinates and $D_s = 27.6^\circ$, $I_s = 44.1^\circ$ with
46 $k_s = 9.0$, $\alpha_{95} = 4.8$, and $D_s = 191.3^\circ$, $I_s = 41.2^\circ$ with $k_s = 5.9$, $\alpha_{95} = 7.4$ in tilt-corrected coordinates,
47 respectively (Figure S3), where D is declination, I is inclination, k is the precision parameter, and
48 α_{95} is the radius that the mean direction lies within 95% confidence (Fisher, 1953). The
49 paleomagnetic reversal test was used to assess whether the average normal pole and reversed pole
50 are statistically antipodal within a given confidence limit (Mcfadden & Mcelhinny, 1990).

51

52 **Text S2** Anisotropy of magnetic susceptibility (AMS) analyses

53 Combined spatial and geometric configuration of the components in a rock is termed petro-fabric
54 or rock fabric and can comprise aspects including lineation, foliation, and grain size which provide
55 important clues for understanding magma flow direction in igneous rocks, paleocurrent flow
56 direction in sedimentary rocks and tectonic strain imparted to metamorphic or otherwise deformed
57 rocks (Ellwood, 1978; Fossen, 2010; Kent & Lowrie, 1975). The AMS method can determine the
58 internal petro-fabric efficiently and relatively rapidly from the preferred orientation of paramagnetic
59 and ferromagnetic grains. Three types of AMS fabrics are defined: the AMS in multi domain
60 magnetite grains is dominated by shape anisotropy with the geometric long axis parallel to the easy
61 axis of magnetization (K1). In rocks dominated by multi domain magnetite, K1 is parallel to the
62 structural lineation and K3 is perpendicular to the foliation; this is defined as a normal magnetic
63 fabric.

64 AMS analyses were tested by AGICO Kappabridge (KLY-4S) in the PGL. The AMS is
65 mathematically described as a second rank tensor and generally visualized by an ellipsoid with three
66 principal eigenvectors, $K_1 > K_2 > K_3$. The maximum principal axis (K_1) defines the lineation; the
67 minimum principal axis (K_3) is perpendicular to the foliation defined by the maximum (K_1) and
68 intermediate (K_2) principal axes (Cañón-Tapia, 1994).

69

70 **Text S3** Detrital Zircons U-Pb Ages test

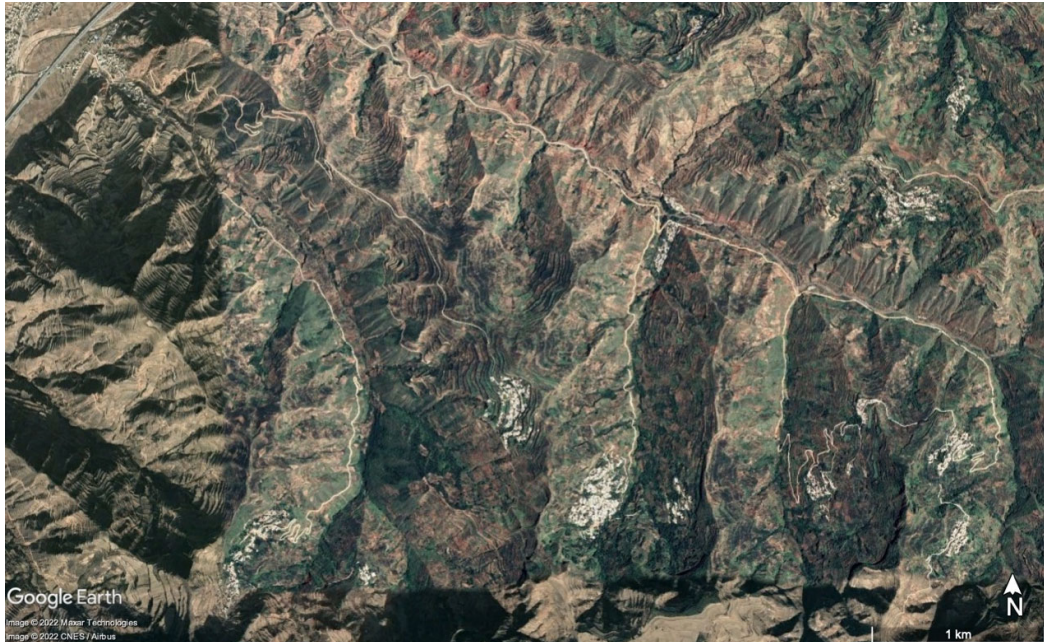
71 More than 5 kg of sandstones for each of the four samples were taken from a single outcrop. Zircon
72 crystals were extracted from sandstone samples following standard water table, magnetic and
73 density separation procedures. Individual zircon crystals (generally more than 300 grains) were
74 mounted into epoxy resin randomly to avoid sampling bias, then approximately 105 grains were
75 randomly dated for each of the samples. Zircon U-Pb dating was carried out at the State Key
76 Laboratory of Earthquake Dynamics, Institute of Geology, China Earthquake Administration, by an
77 Agilent 7900 ICP-MS coupled with a 193 nm excimer laser-ablation system of a Resolution M50-
78 LR. All samples were analyzed using a laser spot size of 40 μm , a frequency of 10 Hz and laser
79 energy density of 4.0 J/cm². To determine fractionation factors and correct for instruments drift, two
80 standards (91500 and GJ-1) were analyzed every 10 grains. As for elements concentration analysis,
81 NIST610 was external standard and ²⁹Si was the internal standard. ICPMSDataCal software was
82 used to calculate the isotope ratios and element contents (Liu et al., 2008). The common lead
83 correction followed the method described by Andersen (2002). Ages younger than ca. 1000 Ma are
84 based on corrected ²⁰⁶Pb/²³⁸U ratio, whereas ages older than ca. 1000 Ma are based on corrected
85 ²⁰⁷Pb/²⁰⁶Pb ratio (Gehrels et al., 2006). Before plotting, we used a moderate discordance filter (10%)

86 to remove highly discordant grains. All reported errors in this study are 1σ . All of the 457 results
87 that yield isotopic data with acceptable discordance and uncertainty are listed in supporting
88 information Table A3.

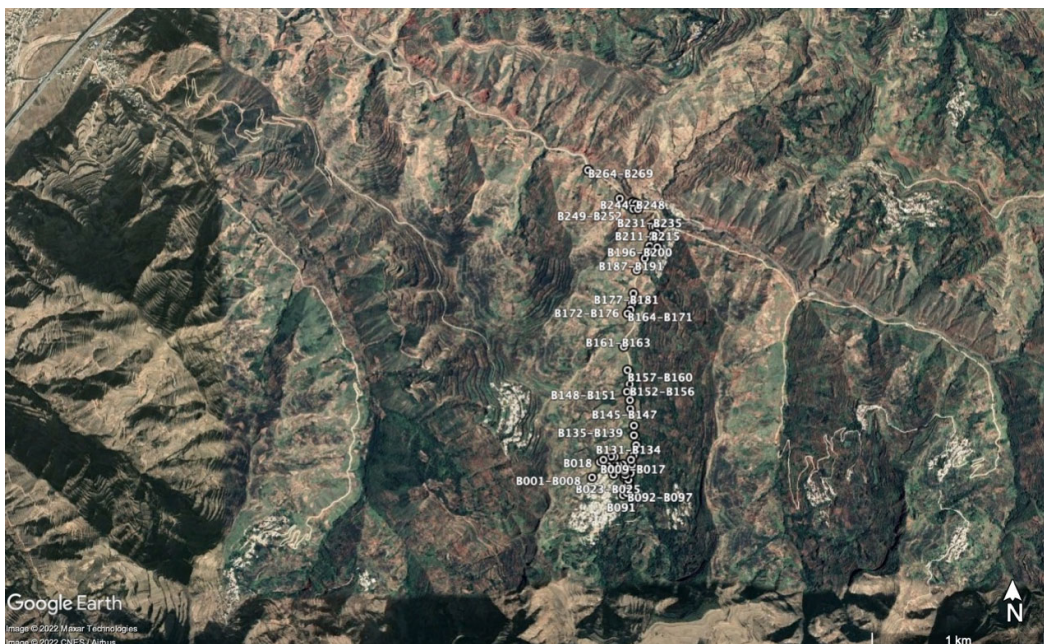
89

90

Figure S1. Anhua sampling section(33°28.32'N 105°01.38'E).



91



92

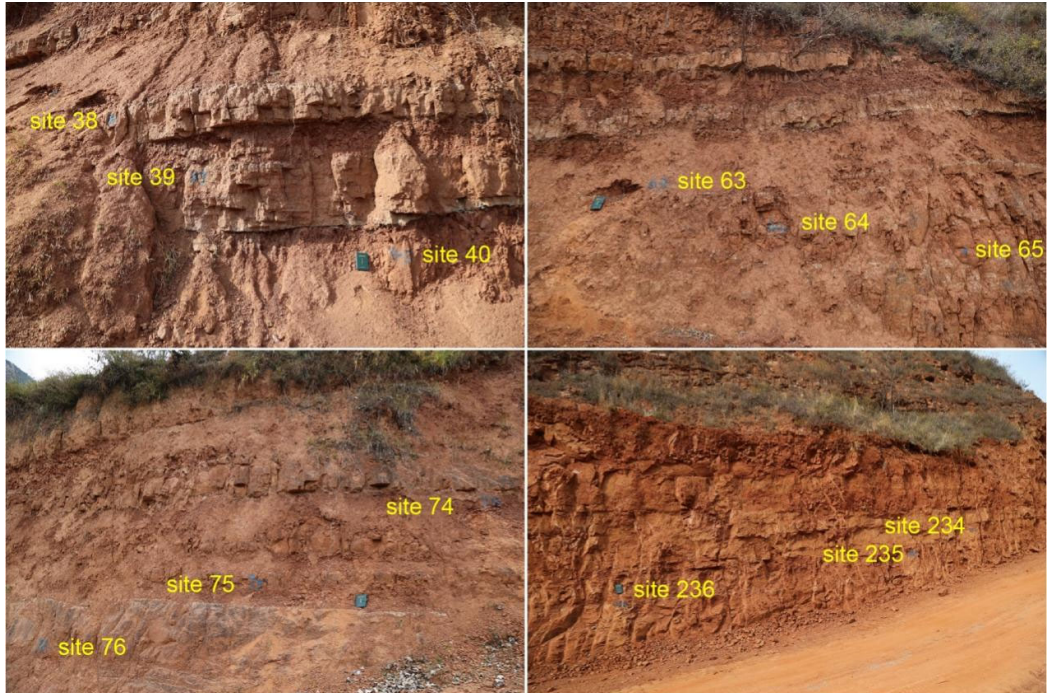


93

94

95

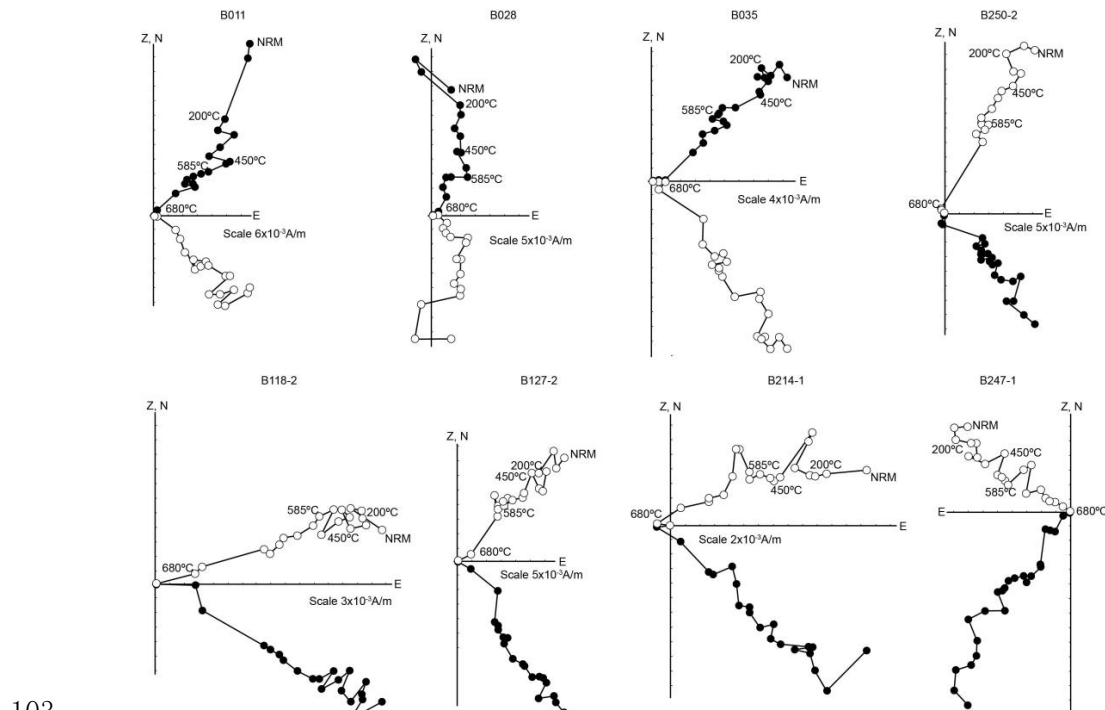
Figure S2. Photographs of the sampled Anhua-Huicheng basin section.



96

97

98 **Figure S3.** Orthogonal (Zijderveld) vector plots of the representative thermal demagnetization
 99 behaviors of specimens from the Anhua section. The hollow (solid) circles show the declination
 100 (inclination) within the orthogonal demagnetization diagrams. NRM is the natural remanent
 101 magnetization before demagnetization, and the numbers mark the temperature steps of
 102 demagnetization.

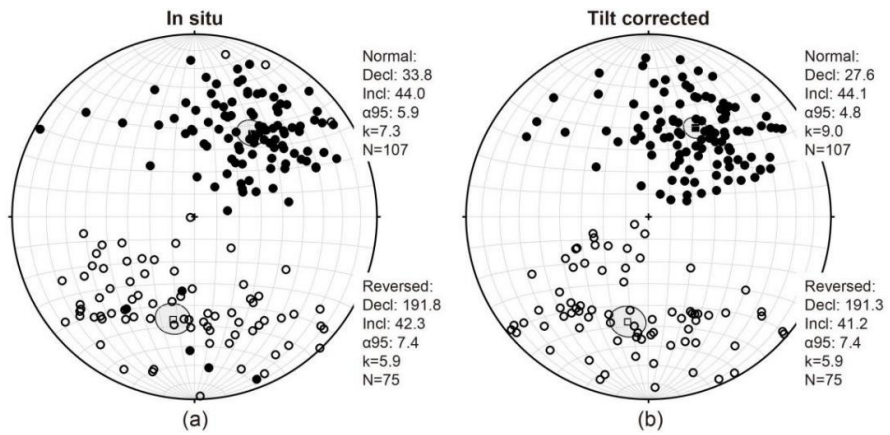


103

104

105 **Figure S4.** Equal-area plots of accepted ChRMs (185 sites) from the Anhua section in (a) geographic
 106 and (b) tilt-corrected coordinates. In the Figures 10(a) and 10(b), hollow (solid) circles plot in the
 107 lower (upper) hemisphere. The ovals indicate the α_{95} error around the Fisher's mean with the mean
 108 data.

109



110 **Figure S5.** AMS data. (a) Equal-area, lower-hemisphere projection of anisotropy of the maximum
111 (blue squares), medium (green triangles) and minimum (pink circles) susceptibility axes in
112 stratigraphic coordinates. (b) P_J-T (corrected degrees of anisotropy vs. shape parameter). (c) Flinn
113 diagram.
114
115

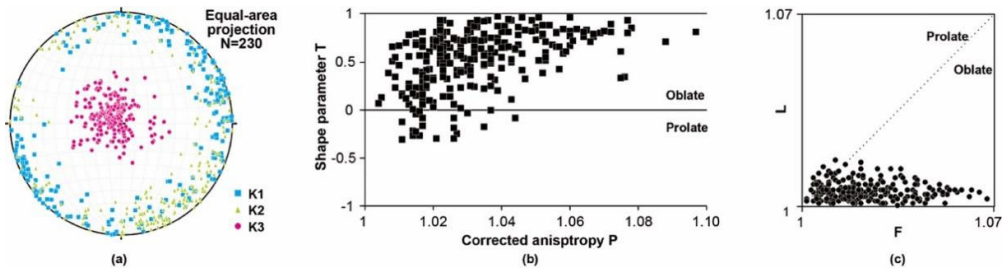


Table S1. Lithofacies and interpretations used in this study.

Lithofacies code	Description	Interpretation
Gms	Structureless, massive, matrix supported gravel	Debris flow deposits
Gma	Poorly sorted, pebble to cobbles conglomerates; matrix -support; fining-up pattern sequence	Gravity flow or braided river lag deposits
Gmb	Poorly sorted, pebble to cobbles conglomerates; matrix support; coarsening-up pattern sequence	Gravity flow deposits
Gcm	Poorly sorted massive pebble conglomerates interbedded with fine sandstone	Debris flow deposits
Gh	Structureless, poorly sorted, pebble-cobbles conglomerates	Sheet flood deposits
Gt	Poorly sorted layered conglomerate with trough and cross-stratification	Braided channel deposits
Gb	Poorly sorted, clast-supported pebble to boulder conglomerates with cross-stratification	Longitudinal bars
Gp	Stratified gravel interbedded with sandstone with planar cross-stratification; matrix- and clast support	Longitudinal bars or deltaic growths from older bar remnants
Gs	Poorly sorted massive sandstone to conglomerate	Debris flow or longitudinal bars or lag deposits
Sm	Structureless, fine to coarse sandstone, may be pebbly	Upper flow regime
Sh	Fine to coarse sandstone, may be pebbly, with horizontal lamination, parting or streaming lineation	Planar bed flow (lower and upper flow regime)
St	Medium to very coarse sandstone, may be pebbly, with cross-stratification	Dunes (lower flow regime)
Sl	Fine sandstone, may be with sandy conglomerate lens pebbly, with low angle cross-stratification	Alluvial fan braided channel/ fan delta/ underwater distributary channel
Sr	Very fine to coarse sandstone with ripple	Lower flow regime
Sc	Fine sandstone with cross-stratification	Lower flow regime

Se	Erosional scours with intra-clasts with crude cross-stratification	Scour fills
Fl	Laminated, sand, silt, mud with small ripples	Overbank or waning flood deposits
Fm	Massive mud and silt	Braided river (middle reaches) or overbank or drape deposits/ lacustrine deposits
Ml	Laminated mud	lacustrine deposits
Mm	Massive mud	overbank or lacustrine deposits
E	Layered gypsum beds	Chemical precipitation in an evaporative lake

Note: Modified after Miall (1978) and DeCelles et al. (1991).

Table S2. Fossils were discovered along the West Qinling Belt.

Location	Fossils	Age
Anhua-Huicheng Basin	<i>Hipparium platyodus</i> , <i>Gazella gaudryi</i> , <i>Acerorhinus</i> , <i>Testudo</i> sp., <i>Dryopithecus wuduensis</i> , <i>Eomellivora</i> sp., <i>Plihyaena</i> sp., <i>Machaerodus fossili</i> , <i>Paramachaerodus</i> sp., <i>Chalicotherium wuduensis</i> , <i>Acerorhinus</i> sp., <i>Chleuastochoerus stehlini</i> , <i>Hanatherium schlosseri</i> , <i>Samotherium</i> sp., <i>Eostyloceras</i> <i>blainvillei</i> , <i>Ceravitus demissus</i> , <i>Metacervulus bidens</i> .	Miocene
Lintan Basin	<i>Eucypris</i> sp., <i>Darwinula</i> sp., <i>Cypris</i> sp., <i>Planorbarius</i> sp., <i>Hippeudis</i> sp.	Miocene
Zeku Basin	<i>Notonectidae</i> sp., <i>Corixidae</i> sp., <i>Cercis</i> sp., <i>Acer subginnala</i> , <i>Typha latissima</i> , <i>Phragmites oenningensis</i> , <i>Phragmites oenin gensis yperacites</i> sp.	Oligocene-Miocene
Wushan Basin	<i>Gomphotherium wimani</i> .	Miocene
Linxia Basin	Hewangjia formation (3.4-5.2 Ma): <i>Hipparium</i> sp. Dongxiang formation (5.2-9 Ma): Giraffidae gen. et sp. indet.; Longguan fauna: <i>Machaerodus</i> (<i>Epimachaerodus</i> ?) cf. <i>ultimus</i> , <i>Indarctos</i> sp., <i>Ictitherium gaudryi</i> , <i>Adcrocuta</i> cf. <i>eximia variabilis</i> , <i>Hipparium</i> (<i>Hipparium</i>) <i>platyodus</i> , <i>H.(H.)</i> <i>fossatum</i> , <i>Hipparium</i> (<i>Cremohipparium</i>) cf. <i>licenti</i> , <i>Acerorhinus linxiaensis</i> sp. nov., <i>A. palaeosinensis</i> , <i>Chilotherium</i> (<i>Chilotherium</i>) <i>anderssoni</i> , <i>C. gracile</i> , <i>Gazella gaudryi</i> , <i>Antilope</i> sp., <i>Cervavitus</i> <i>novorossiae</i> , <i>Propotamochoerus</i> sp. Tala formation (29Ma): <i>Dzungariotherium orgosense</i> , <i>Paraentelodon macrognathus</i> sp. nov.	Pliocene-Oligocene

Data are derived from the following: Anhua-Huicheng Basin: Zhang and Xue (1994); Lintan Basin: GBGMR (1971); Zeku Basin: QBGMR (1971); Wushan Basin: S. Q. Wang et al. (2013); Z. Wang et al. (2012); Linxia Basin: Fang et al. (2003); Li et al. (1980); Qiu et al. (1990).

Table S3. Zircon U-Pb geochronological analyses.

Z1													
Analysis spot	Th/U	$^{207}\text{Pb}/^{235}\text{U}$	1 σ	$^{206}\text{Pb}/^{238}\text{U}$	1 σ	$^{208}\text{Pb}/^{232}\text{Th}$	1 σ	$^{207}\text{Pb}/^{206}\text{Pb}$	1 σ	$^{207}\text{Pb}/^{235}\text{U}$	1 σ	$^{206}\text{Pb}/^{238}\text{U}$	1 σ
1	0.53	0.5523	0.0141	0.0685	0.0015	0.0216	0.0004	561	48	447	9	427	9
2	0.51	0.2551	0.0061	0.0359	0.0008	0.0113	0.0002	289	50	231	5	228	5
3	1.09	1.3034	0.0401	0.1386	0.0030	0.0412	0.0008	830	48	847	18	837	17
4	0.76	5.1649	0.1350	0.3403	0.0072	0.0946	0.0018	1793	37	1847	22	1888	35
5	1.49	1.2548	0.0594	0.1371	0.0031	0.0435	0.0009	960	62	826	27	828	17
6	0.93	1.2682	0.0391	0.1468	0.0031	0.0452	0.0009	736	49	832	18	883	18
7	0.69	5.3397	0.1236	0.3446	0.0073	0.0614	0.0011	1844	36	1875	20	1909	35
8	0.47	0.9791	0.0284	0.1149	0.0025	0.0340	0.0007	647	49	693	15	701	14
9	0.44	0.2407	0.0062	0.0358	0.0008	0.0112	0.0002	250	54	219	5	227	5
10	0.72	1.0015	0.0306	0.1135	0.0024	0.0304	0.0006	750	50	705	16	693	14
11	0.39	2.9789	0.0789	0.2448	0.0052	0.0703	0.0014	1303	40	1402	20	1412	27
12	0.24	6.0282	0.1736	0.3398	0.0072	0.1125	0.0023	2088	36	1980	25	1886	35
13	0.76	0.3984	0.0107	0.0528	0.0011	0.0153	0.0003	435	52	341	8	332	7
14	0.72	1.2305	0.0295	0.1398	0.0030	0.0428	0.0008	754	44	815	13	844	17
15	0.80	1.3017	0.0370	0.1421	0.0030	0.0420	0.0008	782	47	847	16	857	17
16	1.11	1.4028	0.1657	0.1509	0.0042	0.0531	0.0017	838	130	890	70	906	23
17	0.71	4.2449	0.0987	0.2983	0.0063	0.0845	0.0016	1700	37	1683	19	1683	31
18	1.23	1.3712	0.0392	0.1394	0.0030	0.0455	0.0009	995	45	877	17	841	17
19	1.12	1.1269	0.0357	0.1330	0.0028	0.0396	0.0008	803	50	766	17	805	16

20	0.45	0.6385	0.0139	0.0687	0.0015	0.0269	0.0005	911	42	501	9	428	9
21	0.50	0.5206	0.0120	0.0687	0.0015	0.0208	0.0004	425	46	426	8	428	9
22	1.41	1.1111	0.0434	0.1239	0.0027	0.0355	0.0007	811	57	759	21	753	15
23	0.21	5.5400	0.1348	0.3532	0.0074	0.1005	0.0019	1842	36	1907	21	1950	35
24	0.72	0.2827	0.0068	0.0352	0.0007	0.0110	0.0002	546	48	253	5	223	5
25	0.22	0.8959	0.0199	0.0847	0.0018	0.0489	0.0009	1109	41	650	11	524	11
26	0.42	0.2781	0.0074	0.0362	0.0008	0.0121	0.0002	433	53	249	6	229	5
27	0.80	1.2868	0.0390	0.1391	0.0030	0.0412	0.0008	815	48	840	17	839	17
28	0.74	9.9952	0.2341	0.4590	0.0096	0.1218	0.0022	2433	33	2434	22	2435	43
29	0.44	0.5845	0.0158	0.0753	0.0016	0.0241	0.0005	457	51	467	10	468	10
30	0.36	0.3140	0.0077	0.0354	0.0008	0.0144	0.0003	783	47	277	6	225	5
31	7.56	4.8335	0.1828	0.3223	0.0069	0.0947	0.0017	1822	40	1791	32	1801	34
32	0.81	1.1958	0.0599	0.1382	0.0031	0.0434	0.0010	734	68	799	28	834	17
33	0.75	0.5732	0.0155	0.0611	0.0013	0.0225	0.0004	881	48	460	10	383	8
34	0.84	0.5549	0.0155	0.0713	0.0015	0.0235	0.0005	555	52	448	10	444	9
35	0.92	0.5567	0.0136	0.0741	0.0016	0.0225	0.0004	400	48	449	9	461	9
36	1.79	1.3659	0.0436	0.1460	0.0031	0.0419	0.0008	760	49	874	19	879	17
37	0.45	0.2456	0.0062	0.0354	0.0008	0.0112	0.0002	261	53	223	5	224	5
38	0.68	1.2257	0.0360	0.1382	0.0029	0.0404	0.0008	758	48	812	16	834	17
39	0.43	14.1957	0.3290	0.5375	0.0112	0.1443	0.0027	2728	32	2763	22	2773	47
40	0.59	0.9702	0.0287	0.1107	0.0023	0.0331	0.0007	695	50	689	15	677	14
41	1.02	0.6378	0.0152	0.0665	0.0014	0.0220	0.0004	934	44	501	9	415	8

42	0.83	1.1355	0.0346	0.1296	0.0027	0.0391	0.0008	691	50	770	16	786	16
43	0.56	1.4565	0.0387	0.1553	0.0033	0.0461	0.0009	896	44	913	16	930	18
44	0.60	1.1205	0.0351	0.1255	0.0027	0.0386	0.0008	807	50	763	17	762	15
45	1.84	1.1824	0.0310	0.1367	0.0029	0.0420	0.0008	710	46	792	14	826	16
46	0.97	0.3528	0.0106	0.0472	0.0010	0.0143	0.0003	361	59	307	8	297	6
47	0.58	1.3090	0.0360	0.1356	0.0029	0.0420	0.0008	916	45	850	16	820	16
48	0.91	2.0566	0.0608	0.1995	0.0042	0.0549	0.0010	1030	44	1135	20	1172	23
49	0.30	0.6192	0.0154	0.0811	0.0017	0.0255	0.0005	397	49	489	10	503	10
50	0.84	4.7558	0.2243	0.3138	0.0068	0.1008	0.0020	1813	43	1777	40	1759	33
51	0.24	0.5537	0.0124	0.0760	0.0016	0.0236	0.0005	388	46	447	8	472	9
52	0.55	1.3022	0.0320	0.1445	0.0030	0.0426	0.0008	821	44	847	14	870	17
53	0.53	0.2779	0.0083	0.0389	0.0008	0.0121	0.0003	276	61	249	7	246	5
54	1.15	1.1580	0.0327	0.1293	0.0027	0.0380	0.0007	711	48	781	15	784	16
55	0.69	10.8373	0.2720	0.4793	0.0100	0.1315	0.0024	2462	34	2509	23	2524	44
56	0.45	12.3049	0.2998	0.5023	0.0105	0.1358	0.0025	2627	33	2628	23	2624	45
57	0.12	5.6519	0.1251	0.3474	0.0072	0.1025	0.0019	1948	35	1924	19	1922	35
58	0.87	0.7393	0.0193	0.0905	0.0019	0.0273	0.0005	565	49	562	11	559	11
59	0.88	1.1333	0.0372	0.1295	0.0027	0.0375	0.0007	757	51	769	18	785	16
60	0.57	5.3600	0.1482	0.3388	0.0071	0.0953	0.0018	1821	37	1879	24	1881	34
61	0.42	0.3148	0.0091	0.0359	0.0008	0.0139	0.0003	733	54	278	7	227	5
62	0.08	4.7889	0.1529	0.3140	0.0066	0.0901	0.0019	1811	38	1783	27	1760	32
63	0.19	5.7599	0.1226	0.3600	0.0075	0.1200	0.0022	1907	35	1940	18	1982	35

64	0.13	0.6843	0.0145	0.0760	0.0016	0.0397	0.0007	821	42	529	9	472	9
65	1.01	1.1261	0.0352	0.1295	0.0027	0.0391	0.0007	713	50	766	17	785	16
66	0.16	1.2703	0.0321	0.1401	0.0029	0.0458	0.0009	797	45	833	14	845	17
67	0.50	9.7831	0.2647	0.4551	0.0095	0.1199	0.0022	2425	34	2415	25	2418	42
68	0.70	12.4212	0.4019	0.5066	0.0106	0.1351	0.0025	2677	34	2637	30	2642	45
69	0.51	7.6878	1.0907	0.3962	0.0113	0.1569	0.0060	2623	69	2195	127	2152	52
70	0.71	1.1614	0.0442	0.1359	0.0029	0.0394	0.0008	708	56	783	21	821	16
71	0.28	2.1528	0.0528	0.1998	0.0041	0.0606	0.0011	1157	41	1166	17	1174	22
72	1.39	5.6113	0.1971	0.3515	0.0074	0.0979	0.0018	2001	38	1918	30	1942	35
73	1.28	1.2550	0.0432	0.1374	0.0029	0.0401	0.0008	815	52	826	19	830	16
74	0.64	10.5328	0.3937	0.4648	0.0098	0.1275	0.0025	2525	35	2483	35	2461	43
75	0.67	9.8235	0.2851	0.4596	0.0096	0.1303	0.0024	2510	34	2418	27	2438	42
76	0.40	0.6020	0.0128	0.0734	0.0015	0.0232	0.0004	623	44	479	8	457	9
77	0.79	0.5547	0.0149	0.0715	0.0015	0.0217	0.0004	448	51	448	10	445	9
78	1.20	0.7233	0.0236	0.0924	0.0020	0.0286	0.0005	575	56	553	14	569	11
79	0.24	1.4650	0.0362	0.1518	0.0032	0.0438	0.0008	923	43	916	15	911	18
80	0.36	5.3961	0.1206	0.3481	0.0072	0.1075	0.0019	1867	36	1884	19	1925	34
81	0.26	10.4710	0.2536	0.4668	0.0096	0.1331	0.0025	2482	34	2477	22	2470	42
82	1.00	9.6723	0.2528	0.4513	0.0093	0.1173	0.0021	2433	34	2404	24	2401	41
83	1.43	0.4409	0.0166	0.0443	0.0010	0.0142	0.0003	1085	61	371	12	280	6
84	0.75	1.2221	0.0311	0.1328	0.0028	0.0406	0.0008	813	45	811	14	804	16
85	1.10	0.5810	0.0145	0.0589	0.0012	0.0187	0.0003	963	45	465	9	369	7

86	0.65	0.8462	0.0246	0.1054	0.0022	0.0315	0.0006	669	50	623	14	646	13
87	0.20	5.4163	0.1335	0.3425	0.0071	0.0949	0.0018	1858	36	1887	21	1899	34
88	0.66	5.0034	0.1242	0.3258	0.0067	0.0897	0.0016	1831	37	1820	21	1818	33
89	0.47	0.7050	0.0174	0.0520	0.0011	0.0288	0.0005	1611	41	542	10	327	7
90	0.25	1.6580	0.0376	0.1726	0.0036	0.0470	0.0009	939	42	993	14	1026	20
91	1.45	1.6149	0.0388	0.1673	0.0035	0.0489	0.0009	939	43	976	15	997	19
92	1.53	1.1992	0.0608	0.1387	0.0030	0.0422	0.0009	808	67	800	28	838	17
93	1.63	1.0163	0.0345	0.1189	0.0025	0.0369	0.0007	666	54	712	17	724	14
94	0.77	0.5544	0.0206	0.0709	0.0015	0.0212	0.0004	480	65	448	13	442	9
95	0.44	1.6010	0.0362	0.1658	0.0034	0.0470	0.0009	965	42	971	14	989	19
96	0.89	6.6057	0.2479	0.3756	0.0078	0.1036	0.0019	1998	38	2060	33	2056	37
97	0.57	1.4682	0.0494	0.1620	0.0034	0.0462	0.0009	895	50	917	20	968	19
98	0.63	1.2158	0.0418	0.1166	0.0024	0.0400	0.0008	1013	51	808	19	711	14
99	0.47	0.2468	0.0063	0.0353	0.0007	0.0113	0.0002	263	54	224	5	224	5
100	0.99	0.7813	0.0192	0.0905	0.0019	0.0252	0.0005	713	46	586	11	559	11
101	0.53	0.5183	0.0130	0.0688	0.0014	0.0201	0.0004	437	50	424	9	429	9
102	0.89	0.6180	0.0136	0.0734	0.0015	0.0234	0.0004	644	45	489	9	457	9
103	0.49	0.2429	0.0061	0.0348	0.0007	0.0107	0.0002	217	54	221	5	220	4
104	0.38	10.6689	0.2431	0.4682	0.0096	0.1302	0.0023	2529	33	2495	21	2476	42
105	0.60	1.1620	0.0533	0.1258	0.0027	0.0379	0.0009	853	63	783	25	764	15
106	0.80	1.1360	0.0470	0.1259	0.0027	0.0370	0.0008	751	60	771	22	765	15
107	0.91	1.2640	0.0328	0.1412	0.0029	0.0401	0.0007	816	45	830	15	851	16

108	0.11	2.1947	0.0451	0.1577	0.0032	0.0615	0.0011	1675	37	1179	14	944	18	
109	0.62	0.2424	0.0070	0.0348	0.0007	0.0108	0.0002	312	59	220	6	220	5	
110	0.40	0.5559	0.0131	0.0336	0.0007	0.0246	0.0005	2000	39	449	9	213	4	
111	0.71	1.0895	0.2372	0.1169	0.0054	0.0258	0.0026	1510	225	748	115	713	31	
112	0.67	0.5479	0.0141	0.0714	0.0015	0.0215	0.0004	434	50	444	9	445	9	
113	0.54	0.2472	0.0064	0.0362	0.0008	0.0110	0.0002	193	56	224	5	229	5	
114	0.55	1.1944	0.0361	0.1311	0.0027	0.0393	0.0008	819	49	798	17	794	15	
115	0.84	1.3175	0.0312	0.1433	0.0029	0.0473	0.0008	822	44	853	14	863	17	
116	0.12	0.3034	0.0064	0.0359	0.0007	0.0196	0.0004	682	44	269	5	227	5	
117	0.39	1.4400	0.0313	0.1483	0.0030	0.0466	0.0008	972	41	906	13	891	17	
118	0.73	1.9712	0.0427	0.1887	0.0038	0.0572	0.0010	1118	40	1106	15	1115	21	
119	0.99	0.3141	0.0081	0.0434	0.0009	0.0137	0.0003	300	54	277	6	274	6	
120	0.54	0.5476	0.0151	0.0720	0.0015	0.0216	0.0004	419	52	443	10	448	9	

Z2														
Analysis spot	Th/U	$^{207}\text{Pb}/^{235}\text{U}$	1 σ	$^{206}\text{Pb}/^{238}\text{U}$	1 σ	$^{208}\text{Pb}/^{232}\text{Th}$	1 σ	$^{207}\text{Pb}/^{206}\text{Pb}$	1 σ	$^{207}\text{Pb}/^{235}\text{U}$	1 σ	$^{206}\text{Pb}/^{238}\text{U}$	1 σ	
1	0.87	1.1855	0.0483	0.1335	0.0027	0.0438	0.0009	732	59	794	22	808	16	
2	1.44	0.5378	0.0175	0.0712	0.0014	0.0227	0.0004	359	60	437	12	444	9	
3	0.82	21.2401	0.5169	0.6277	0.0124	0.1627	0.0029	3094	32	3150	24	3140	49	
4	0.81	0.5491	0.0141	0.0724	0.0014	0.0222	0.0004	427	50	444	9	451	9	
5	0.39	0.2423	0.0071	0.0348	0.0007	0.0110	0.0002	165	62	220	6	221	4	
6	0.84	10.7364	0.2943	0.4743	0.0094	0.1342	0.0025	2461	34	2501	25	2503	41	

7	1.20	1.1458	0.0416	0.1246	0.0025	0.0353	0.0007	737	55	775	20	757	14
8	1.07	1.2234	0.0425	0.1312	0.0027	0.0399	0.0008	816	52	811	19	795	15
9	0.24	5.3458	0.1200	0.3396	0.0067	0.0952	0.0017	1835	36	1876	19	1885	32
10	0.95	0.9836	0.0225	0.0697	0.0014	0.0297	0.0005	1631	39	695	12	435	8
11	0.77	1.2478	0.0550	0.1344	0.0028	0.0410	0.0009	735	61	822	25	813	16
12	1.62	2.5789	0.0554	0.2232	0.0044	0.0633	0.0011	1278	39	1295	16	1299	23
13	0.40	0.2448	0.0069	0.0347	0.0007	0.0109	0.0002	264	59	222	6	220	4
14	0.66	1.4061	0.0418	0.1185	0.0024	0.0459	0.0009	1330	44	892	18	722	14
15	0.40	0.2583	0.0080	0.0353	0.0007	0.0118	0.0003	298	63	233	6	224	4
16	0.89	1.0997	0.0313	0.1248	0.0025	0.0389	0.0007	717	48	753	15	758	14
17	1.05	1.2611	0.0535	0.1392	0.0029	0.0427	0.0009	805	59	828	24	840	16
18	0.28	0.2459	0.0065	0.0350	0.0007	0.0114	0.0002	230	56	223	5	221	4
19	0.43	0.2905	0.0082	0.0339	0.0007	0.0130	0.0003	665	54	259	6	215	4
20	0.84	0.5269	0.0145	0.0699	0.0014	0.0213	0.0004	377	53	430	10	435	8
21	0.88	0.5343	0.0174	0.0688	0.0014	0.0216	0.0004	519	59	435	12	429	8
22	1.51	0.5148	0.0122	0.0683	0.0014	0.0207	0.0004	385	49	422	8	426	8
23	0.92	0.6928	0.0171	0.0864	0.0017	0.0269	0.0005	509	49	535	10	534	10
24	0.42	0.4075	0.0111	0.0333	0.0007	0.0179	0.0004	1393	46	347	8	211	4
25	0.48	1.5741	0.0372	0.1488	0.0030	0.0450	0.0008	1078	42	960	15	894	17
26	1.17	1.1294	0.0303	0.1272	0.0025	0.0375	0.0007	748	47	768	14	772	15
27	0.38	0.5099	0.0127	0.0650	0.0013	0.0201	0.0004	441	50	418	9	406	8
28	0.58	0.2604	0.0069	0.0362	0.0007	0.0117	0.0002	253	56	235	6	230	5

29	0.95	1.1635	0.0427	0.1282	0.0026	0.0395	0.0008	776	55	784	20	778	15
30	0.72	2.1406	0.0558	0.1972	0.0039	0.0582	0.0011	1156	42	1162	18	1160	21
31	1.09	1.2411	0.0278	0.1321	0.0026	0.0406	0.0007	875	42	819	13	800	15
32	0.60	0.4767	0.0140	0.0348	0.0007	0.0166	0.0003	1662	47	396	10	221	4
33	0.94	1.1451	0.0340	0.1315	0.0026	0.0404	0.0008	738	49	775	16	796	15
34	1.04	1.8505	0.0504	0.1786	0.0036	0.0536	0.0010	1072	43	1064	18	1059	20
35	0.56	10.5572	0.2501	0.4706	0.0093	0.1283	0.0023	2486	34	2485	22	2486	41
36	0.48	0.2570	0.0068	0.0360	0.0007	0.0113	0.0002	243	56	232	6	228	5
37	0.47	0.8338	0.0220	0.0949	0.0019	0.0318	0.0006	721	48	616	12	585	11
38	0.78	1.3257	0.0291	0.1115	0.0022	0.0267	0.0005	1328	40	857	13	681	13
39	0.66	0.5981	0.0157	0.0762	0.0015	0.0220	0.0004	418	51	476	10	473	9
40	0.71	1.1235	0.0394	0.1238	0.0025	0.0388	0.0008	761	54	765	19	753	14
41	0.71	1.4578	0.0375	0.1491	0.0030	0.0453	0.0008	913	44	913	16	896	17
42	1.97	1.1067	0.0366	0.1156	0.0023	0.0318	0.0006	870	51	757	18	705	14
43	1.27	1.1004	0.0249	0.1184	0.0024	0.0345	0.0006	828	43	754	12	722	14
44	0.72	1.3012	0.0414	0.1328	0.0027	0.0392	0.0008	854	49	846	18	804	15
45	0.90	1.1526	0.0611	0.1321	0.0028	0.0400	0.0009	753	71	779	29	800	16
46	0.70	1.2133	0.0419	0.1325	0.0027	0.0395	0.0008	769	53	807	19	802	15
47	0.55	0.4043	0.0117	0.0481	0.0010	0.0158	0.0003	683	54	345	8	303	6
48	0.34	0.2391	0.0063	0.0342	0.0007	0.0104	0.0002	206	56	218	5	217	4
49	0.86	1.5547	0.0350	0.1588	0.0032	0.0490	0.0009	935	42	952	14	950	18
50	0.80	1.2964	0.0337	0.1409	0.0028	0.0438	0.0008	812	45	844	15	850	16

51	0.39	2.7702	0.0587	0.2207	0.0044	0.0739	0.0013	1416	38	1348	16	1286	23
52	0.79	1.2559	0.0333	0.1235	0.0025	0.0396	0.0007	974	45	826	15	751	14
53	0.29	5.3477	0.1259	0.3388	0.0068	0.0953	0.0017	1849	36	1877	20	1881	33
54	0.50	1.2570	0.0320	0.1354	0.0027	0.0408	0.0008	812	45	827	14	819	15
55	0.76	6.4130	0.1740	0.3678	0.0074	0.1044	0.0019	1996	36	2034	24	2019	35
56	0.97	1.0333	0.0400	0.1228	0.0025	0.0363	0.0007	644	59	721	20	747	14
57	0.47	1.5212	0.0349	0.1556	0.0031	0.0465	0.0008	919	42	939	14	932	17
58	0.52	0.2370	0.0071	0.0348	0.0007	0.0103	0.0002	145	63	216	6	220	4
59	0.57	1.1755	0.0298	0.1313	0.0026	0.0397	0.0007	765	45	789	14	795	15
60	0.79	1.2056	0.0397	0.1328	0.0027	0.0402	0.0008	732	52	803	18	804	15
61	1.80	1.6504	0.0402	0.1639	0.0033	0.0478	0.0009	998	43	990	15	978	18
62	0.66	1.5278	0.0383	0.1402	0.0028	0.0388	0.0007	1182	42	942	15	846	16
63	0.87	1.2211	0.0361	0.1293	0.0026	0.0397	0.0007	794	48	810	17	784	15
64	1.58	1.0684	0.0312	0.1186	0.0024	0.0352	0.0006	758	49	738	15	722	14
65	0.67	1.0440	0.0222	0.0978	0.0020	0.0298	0.0005	1139	40	726	11	601	11
66	0.73	1.6023	0.0447	0.1473	0.0030	0.0475	0.0009	1114	44	971	17	886	17
67	0.74	0.9125	0.0234	0.1054	0.0021	0.0316	0.0006	655	47	658	12	646	12
68	0.89	10.9720	0.2736	0.4771	0.0095	0.1307	0.0023	2500	34	2521	23	2515	42
69	0.44	0.2328	0.0070	0.0346	0.0007	0.0108	0.0002	171	63	213	6	219	4
70	0.36	0.5979	0.0152	0.0717	0.0014	0.0218	0.0004	631	49	476	10	446	9
71	1.51	1.1983	0.0279	0.1324	0.0027	0.0383	0.0007	816	44	800	13	802	15
72	1.57	1.2063	0.0403	0.1312	0.0027	0.0386	0.0007	790	52	804	19	795	15

73	0.69	0.8683	0.0335	0.1071	0.0022	0.0318	0.0007	624	61	635	18	656	13
74	0.55	0.6998	0.0170	0.0871	0.0018	0.0257	0.0005	516	48	539	10	538	10
75	0.32	2.5751	0.0776	0.2170	0.0044	0.0663	0.0013	1251	43	1294	22	1266	23
76	0.51	1.2392	0.0299	0.1270	0.0026	0.0410	0.0008	936	43	819	14	771	15
77	0.50	0.2548	0.0076	0.0348	0.0007	0.0105	0.0002	289	61	230	6	220	4
78	0.96	1.0993	0.0450	0.1239	0.0026	0.0393	0.0008	776	59	753	22	753	15
79	0.47	1.5986	0.0409	0.1618	0.0033	0.0482	0.0009	979	44	970	16	967	18
80	0.89	1.2547	0.0368	0.1322	0.0027	0.0401	0.0008	838	48	826	17	800	15
81	1.22	1.1282	0.0317	0.1247	0.0025	0.0371	0.0007	788	48	767	15	758	14
82	1.11	1.1700	0.0388	0.1264	0.0026	0.0361	0.0007	883	51	787	18	767	15
83	0.78	1.2401	0.0286	0.1315	0.0026	0.0395	0.0007	863	43	819	13	797	15
84	0.58	1.4142	0.0375	0.1455	0.0029	0.0437	0.0008	898	45	895	16	876	16
85	0.92	0.5309	0.0153	0.0692	0.0014	0.0202	0.0004	412	54	432	10	432	8
86	0.87	1.2219	0.0402	0.1305	0.0027	0.0385	0.0007	785	51	811	18	790	15
87	0.92	1.1578	0.0450	0.1278	0.0026	0.0377	0.0008	718	58	781	21	775	15
88	0.70	0.2346	0.0069	0.0333	0.0007	0.0102	0.0002	236	61	214	6	211	4
89	2.15	1.0818	0.0242	0.1213	0.0024	0.0364	0.0006	757	44	745	12	738	14
90	0.89	1.3107	0.0314	0.1417	0.0029	0.0416	0.0008	842	44	850	14	854	16
91	0.55	1.3573	0.0464	0.1491	0.0030	0.0519	0.0010	792	52	871	20	896	17
92	0.33	0.2550	0.0075	0.0350	0.0007	0.0110	0.0002	249	61	231	6	222	4
93	0.95	1.7545	0.0456	0.1648	0.0033	0.0527	0.0010	1103	43	1029	17	983	18
94	0.43	0.2883	0.0090	0.0345	0.0007	0.0128	0.0003	650	60	257	7	218	4

95	0.94	1.2122	0.0377	0.1323	0.0027	0.0401	0.0008	786	50	806	17	801	15
96	1.08	1.1531	0.0374	0.1239	0.0025	0.0359	0.0007	714	52	779	18	753	14
97	0.95	1.2466	0.0304	0.1343	0.0027	0.0391	0.0007	841	44	822	14	813	15
98	0.80	5.8341	0.2005	0.3542	0.0072	0.0988	0.0018	2017	38	1952	30	1955	34
99	1.18	10.7677	0.3007	0.4727	0.0095	0.1294	0.0023	2492	34	2503	26	2496	42
100	1.14	1.1065	0.0292	0.1233	0.0025	0.0357	0.0007	749	47	757	14	750	14
101	1.10	0.9117	0.0491	0.0684	0.0015	0.0192	0.0005	1576	68	658	26	427	9
102	1.04	1.1224	0.0485	0.1053	0.0022	0.0369	0.0008	1084	59	764	23	645	13
103	0.27	1.8365	0.0634	0.1764	0.0036	0.0526	0.0012	1053	48	1059	23	1047	20
104	1.24	1.2250	0.0458	0.1288	0.0027	0.0382	0.0007	842	55	812	21	781	15
105	0.67	0.2605	0.0081	0.0336	0.0007	0.0099	0.0002	413	61	235	7	213	4
106	0.46	9.9090	0.2451	0.4555	0.0092	0.1271	0.0023	2433	34	2426	23	2420	41
107	0.90	0.3374	0.0085	0.0292	0.0006	0.0110	0.0002	1309	45	295	6	186	4
108	0.52	1.2977	0.0368	0.1355	0.0028	0.0401	0.0008	836	47	845	16	819	16
109	1.03	1.1898	0.0454	0.1283	0.0027	0.0383	0.0008	801	56	796	21	778	15
110	0.86	1.0578	0.0337	0.1210	0.0025	0.0363	0.0007	746	52	733	17	736	14
111	0.81	1.4686	0.0342	0.1337	0.0027	0.0409	0.0007	1181	41	918	14	809	15
112	0.14	1.1798	0.0287	0.1220	0.0025	0.0384	0.0008	911	44	791	13	742	14
113	0.76	0.3230	0.0139	0.0337	0.0007	0.0122	0.0003	966	74	284	11	214	5
114	2.53	1.1044	0.0386	0.1249	0.0026	0.0378	0.0007	800	54	756	19	759	15
115	0.90	1.1528	0.0386	0.1218	0.0025	0.0363	0.0007	857	52	779	18	741	14
116	0.25	1.5915	0.0398	0.1610	0.0033	0.0496	0.0010	1018	43	967	16	962	18

117	0.19	5.8364	0.1357	0.3517	0.0071	0.0590	0.0011	1961	36	1952	20	1943	34
118	0.72	1.8881	0.0568	0.1797	0.0037	0.0589	0.0011	1110	45	1077	20	1065	20
119	0.90	1.0890	0.0390	0.1163	0.0024	0.0347	0.0007	845	54	748	19	709	14
120	0.35	0.2541	0.0079	0.0359	0.0007	0.0112	0.0002	168	65	230	6	227	5

Z3													
Analysis spot	Th/U	$^{207}\text{Pb}/^{235}\text{U}$	1 σ	$^{206}\text{Pb}/^{238}\text{U}$	1 σ	$^{208}\text{Pb}/^{232}\text{Th}$	1 σ	$^{207}\text{Pb}/^{206}\text{Pb}$	1 σ	$^{207}\text{Pb}/^{235}\text{U}$	1 σ	$^{206}\text{Pb}/^{238}\text{U}$	1 σ
1	0.25	10.3423	1.1202	0.4610	0.0111	0.1371	0.0053	2508	52	2466	100	2444	49
2	0.65	1.3775	0.0296	0.1367	0.0028	0.0436	0.0009	1165	40	879	13	826	16
3	1.01	0.2102	0.0063	0.0296	0.0006	0.0098	0.0002	353	32	194	5	188	4
4	0.54	8.1970	0.1935	0.4143	0.0086	0.1128	0.0022	2410	34	2253	21	2235	39
5	0.90	1.0214	0.0249	0.1198	0.0025	0.0362	0.0007	803	45	715	13	729	14
6	0.49	1.0409	0.0287	0.1244	0.0026	0.0367	0.0007	819	47	724	14	756	15
7	0.36	0.3626	0.0093	0.0417	0.0009	0.0141	0.0003	904	49	314	7	264	5
8	0.60	4.2074	0.1309	0.2905	0.0061	0.0866	0.0017	1813	39	1676	26	1644	30
9	0.81	1.4367	0.0334	0.1506	0.0031	0.0447	0.0008	998	42	904	14	904	17
10	0.92	1.2158	0.0418	0.1166	0.0024	0.0400	0.0008	1013	51	808	19	711	14
11	0.11	1.2208	0.0312	0.1337	0.0028	0.0432	0.0008	847	45	810	14	809	16
12	0.62	1.4733	0.0304	0.1548	0.0032	0.0623	0.0012	990	41	920	12	928	18
13	0.22	4.3293	0.0990	0.3015	0.0062	0.0840	0.0016	1776	37	1699	19	1699	31
14	0.40	0.4071	0.0099	0.0565	0.0012	0.0175	0.0003	423	49	347	7	354	7
15	0.76	4.1104	0.0978	0.2945	0.0061	0.0856	0.0016	1748	37	1656	19	1664	30

16	0.68	0.6367	0.0194	0.0431	0.0009	0.0226	0.0005	1775	46	500	12	272	6
17	0.56	0.6367	0.0194	0.0431	0.0009	0.0226	0.0005	1776	47	501	13	273	7
18	0.56	1.2221	0.0311	0.1328	0.0028	0.0406	0.0008	813	45	811	14	804	16
19	0.84	0.6645	0.0181	0.0839	0.0017	0.0256	0.0005	530	51	517	11	519	10
20	0.12	5.2764	0.1181	0.3347	0.0069	0.0923	0.0017	1909	36	1865	19	1861	33
21	0.38	4.6293	0.1617	0.3108	0.0063	0.0930	0.0019	1859	39	1755	29	1745	31
22	0.73	1.3378	0.0624	0.1285	0.0027	0.0428	0.0009	878	61	862	27	779	15
23	1.04	1.1020	0.0479	0.1175	0.0025	0.0378	0.0008	945	60	754	23	716	14
24	0.99	4.2028	0.2614	0.2531	0.0054	0.0729	0.0015	1771	50	1675	51	1454	28
25	0.53	10.0240	0.3909	0.4584	0.0093	0.1114	0.0023	2501	35	2437	36	2432	41
26	0.40	1.1653	0.0409	0.1312	0.0027	0.0384	0.0007	752	53	784	19	795	15
27	0.66	0.4904	0.0111	0.0387	0.0008	0.0183	0.0003	1477	41	405	8	245	5
28	0.89	3.7735	0.1028	0.2793	0.0056	0.0817	0.0014	1593	38	1587	22	1588	28
29	0.50	0.4959	0.0131	0.0609	0.0012	0.0188	0.0004	555	51	409	9	381	7
30	0.71	0.9109	0.0205	0.1080	0.0022	0.0376	0.0007	660	44	658	11	661	13
31	1.24	1.1173	0.0296	0.1230	0.0025	0.0364	0.0007	758	46	762	14	748	14
32	1.11	6.2377	0.6313	0.3622	0.0086	0.0886	0.0036	2178	59	2010	89	1993	41
33	1.05	1.1111	0.0289	0.1324	0.0027	0.0398	0.0007	773	46	759	14	802	15
34	0.31	1.5068	0.0371	0.1604	0.0032	0.0475	0.0008	928	43	933	15	959	18
35	0.73	0.4446	0.0089	0.0511	0.0010	0.0136	0.0002	752	42	374	6	321	6
36	0.16	4.9987	0.3193	0.3249	0.0072	0.1136	0.0028	2556	46	1819	54	1814	35
37	0.69	0.6896	0.0144	0.0714	0.0014	0.0377	0.0007	952	41	533	9	445	9

38	1.13	13.2563	0.3116	0.5174	0.0107	0.0857	0.0017	2719	33	2698	22	2688	45	
39	1.15	0.2454	0.0079	0.0332	0.0007	0.0105	0.0002	467	64	223	6	210	4	
40	0.77	1.2016	0.0373	0.1229	0.0025	0.0389	0.0007	998	48	801	17	747	14	
41	1.27	7.4223	0.2909	0.3950	0.0080	0.1110	0.0021	2211	37	2164	35	2146	37	
42	0.74	5.1345	0.1039	0.3207	0.0064	0.0916	0.0016	1926	35	1842	17	1793	31	
43	0.72	0.4941	0.0112	0.0582	0.0012	0.0199	0.0004	717	45	408	8	365	7	
44	0.21	1.1604	0.0286	0.1289	0.0026	0.0377	0.0007	865	44	782	13	782	15	
45	0.15	0.5742	0.0120	0.0697	0.0014	0.0251	0.0005	640	44	461	8	434	8	
46	0.77	1.1485	0.0295	0.1281	0.0026	0.0372	0.0007	778	46	777	14	777	15	
47	0.92	0.5191	0.0109	0.0637	0.0013	0.0186	0.0003	584	44	425	7	398	8	
48	0.21	4.5468	0.2652	0.2999	0.0064	0.0738	0.0017	1862	47	1740	49	1691	31	
49	0.93	0.9713	0.0236	0.1098	0.0022	0.0365	0.0007	772	45	689	12	672	13	
50	1.02	1.9128	0.4684	0.1844	0.0090	0.0522	0.0071	1974	196	1086	163	1091	49	
51	1.30	0.8004	0.0180	0.0992	0.0020	0.0279	0.0011	573	45	597	10	610	12	
52	0.51	1.2852	0.0284	0.1327	0.0027	0.0372	0.0007	965	42	839	13	803	15	
53	0.86	6.0357	0.3828	0.3500	0.0075	0.0905	0.0026	2118	46	1981	55	1935	36	
54	0.42	0.3993	0.0105	0.0413	0.0008	0.0130	0.0002	906	49	341	8	261	5	
55	0.86	0.6350	0.0157	0.0761	0.0015	0.0229	0.0004	667	47	499	10	473	9	
56	0.14	1.9364	0.0455	0.1670	0.0033	0.0470	0.0009	1334	40	1094	16	995	18	
57	0.01	0.2939	0.0068	0.0420	0.0008	0.0128	0.0002	263	50	262	5	265	5	
58	0.85	5.0701	0.8697	0.3270	0.0100	0.0800	0.0049	2116	96	1831	145	1824	49	
59	0.38	0.3528	0.0106	0.0472	0.0010	0.0143	0.0003	361	59	307	8	297	6	

60	1.17	0.4043	0.0117	0.0481	0.0010	0.0158	0.0003	683	54	345	8	303	6
61	0.41	1.2969	0.0290	0.1215	0.0024	0.0332	0.0006	1128	41	844	13	739	14
62	0.49	0.6383	0.0147	0.0750	0.0015	0.0262	0.0005	839	44	501	9	466	9
63	0.42	1.2961	0.0481	0.1447	0.0030	0.0424	0.0009	765	54	844	21	871	17
64	0.65	0.5574	0.0150	0.0646	0.0013	0.0235	0.0004	801	49	450	10	404	8
65	0.38	0.3732	0.0121	0.0430	0.0009	0.0147	0.0003	755	59	322	9	271	5
66	1.18	1.4112	0.0307	0.1488	0.0030	0.0439	0.0008	905	42	894	13	894	17
67	0.56	1.2121	0.0270	0.1325	0.0026	0.0390	0.0007	832	43	806	12	802	15
68	0.01	3.8896	0.1599	0.2895	0.0059	0.0850	0.0016	1596	43	1612	33	1639	30
69	0.87	0.7746	0.0169	0.0971	0.0019	0.0280	0.0010	567	45	582	10	598	11
70	0.69	10.4947	0.2646	0.4701	0.0094	0.1267	0.0022	2476	34	2480	23	2484	41
71	0.56	1.2840	0.0275	0.1376	0.0027	0.0362	0.0007	867	42	839	12	831	15
72	0.97	5.0997	0.1109	0.3312	0.0066	0.0911	0.0016	1841	36	1836	18	1844	32
73	0.86	3.6898	0.0870	0.2750	0.0055	0.0751	0.0013	1588	38	1569	19	1566	28
74	0.48	0.3618	0.0158	0.0436	0.0010	0.0173	0.0005	579	77	314	12	275	6
75	0.27	0.9064	0.0194	0.0949	0.0019	0.0317	0.0006	907	42	655	10	585	11
76	0.62	0.5204	0.0141	0.0689	0.0014	0.0194	0.0004	476	53	425	9	429	8
77	0.38	5.8366	0.1532	0.3496	0.0070	0.0536	0.0010	2051	36	1952	23	1933	33
78	1.05	8.4933	2.6375	0.4314	0.0194	0.1686	0.0105	2536	128	2285	282	2312	87
79	0.01	2.5909	0.0588	0.2264	0.0045	0.0719	0.0013	1296	39	1298	17	1316	24
80	0.60	0.7924	0.0163	0.0888	0.0018	0.0391	0.0007	863	42	593	9	548	10
81	0.69	0.5810	0.0145	0.0589	0.0012	0.0187	0.0003	963	45	465	9	369	7

82	0.07	7.5908	0.1705	0.3968	0.0079	0.1013	0.0018	2212	34	2184	20	2154	36	
83	0.85	1.7284	0.0508	0.1550	0.0031	0.0487	0.0009	1141	44	1019	19	929	17	
84	0.35	8.8313	0.1924	0.4295	0.0085	0.1091	0.0019	2351	34	2321	20	2303	38	
85	0.76	0.3770	0.0094	0.0404	0.0008	0.0139	0.0003	849	48	325	7	255	5	
86	1.44	1.9099	0.3739	0.1835	0.0069	0.0448	0.0034	1617	165	1085	130	1086	38	
87	1.26	0.3634	0.0111	0.0340	0.0007	0.0150	0.0003	1162	53	315	8	216	4	
88	1.10	0.5399	0.0133	0.0699	0.0014	0.0204	0.0004	502	50	438	9	435	8	
89	0.93	1.0684	0.0492	0.1224	0.0026	0.0370	0.0008	883	63	738	24	744	15	
90	0.25	4.5546	0.1079	0.3053	0.0061	0.0830	0.0015	1750	37	1741	20	1717	30	
91	0.84	9.6630	0.2067	0.4515	0.0089	0.1169	0.0020	2406	34	2403	20	2402	40	
92	0.57	0.3560	0.0139	0.0388	0.0008	0.0154	0.0004	841	68	309	10	246	5	
93	0.37	1.1785	0.0256	0.1260	0.0025	0.0372	0.0007	858	42	791	12	765	14	
94	0.51	10.0022	0.2359	0.4537	0.0090	0.1096	0.0020	2490	34	2435	22	2412	40	
95	0.96	2.2002	0.0600	0.2034	0.0041	0.0601	0.0011	1145	42	1181	19	1194	22	
96	0.66	1.1589	0.0289	0.1304	0.0026	0.0346	0.0006	796	45	781	14	790	15	

Z4														
Analysis spot	Th/U	$^{207}\text{Pb}/^{235}\text{U}$	1 σ	$^{206}\text{Pb}/^{238}\text{U}$	1 σ	$^{208}\text{Pb}/^{232}\text{Th}$	1 σ	$^{207}\text{Pb}/^{206}\text{Pb}$	1 σ	$^{207}\text{Pb}/^{235}\text{U}$	1 σ	$^{206}\text{Pb}/^{238}\text{U}$	1 σ	
1	0.48	1.0868	0.0254	0.1034	0.0021	0.0249	0.0005	1051	42	747	12	634	12	
2	0.51	1.1849	0.0263	0.1272	0.0026	0.0377	0.0007	799	43	794	12	772	15	
3	0.48	1.7167	0.0391	0.1706	0.0035	0.0493	0.0009	980	42	1015	15	1015	19	
4	0.45	1.5716	0.0363	0.1587	0.0032	0.0448	0.0009	939	42	959	14	949	18	

5	0.90	1.2296	0.0320	0.1329	0.0027	0.0427	0.0008	850	45	814	15	804	15
6	0.18	1.3041	0.0318	0.1196	0.0024	0.0433	0.0008	1156	42	848	14	728	14
7	0.91	1.9843	0.0448	0.1839	0.0038	0.0523	0.0010	1123	41	1110	15	1088	20
8	0.86	0.3240	0.0096	0.0443	0.0009	0.0142	0.0003	279	59	285	7	280	6
9	0.43	1.9753	0.0472	0.1817	0.0037	0.0561	0.0011	1110	41	1107	16	1076	20
10	0.44	1.3897	0.0368	0.1455	0.0030	0.0477	0.0009	910	45	885	16	876	17
11	1.11	1.3151	0.0298	0.1360	0.0028	0.0434	0.0008	871	43	852	13	822	16
12	0.04	1.6727	0.0374	0.1660	0.0034	0.0576	0.0011	1001	41	998	14	990	19
13	1.04	1.2679	0.0428	0.1311	0.0027	0.0397	0.0008	899	51	831	19	794	16
14	0.32	0.3630	0.0101	0.0446	0.0009	0.0159	0.0003	563	54	314	8	281	6
15	1.03	2.3463	0.0529	0.2131	0.0043	0.0638	0.0012	1120	41	1226	16	1245	23
16	0.41	5.4945	0.1580	0.3444	0.0071	0.1018	0.0020	1816	38	1900	25	1908	34
17	1.88	0.2906	0.0143	0.0401	0.0009	0.0138	0.0004	306	93	259	11	253	5
18	0.94	1.4576	0.0335	0.1407	0.0029	0.0414	0.0008	1067	41	913	14	849	16
19	0.57	7.9097	0.4499	0.4093	0.0088	0.0471	0.0013	2198	42	2221	51	2212	40
20	0.63	1.2781	0.0304	0.1269	0.0026	0.0398	0.0008	944	43	836	14	770	15
21	0.46	0.4405	0.0105	0.0489	0.0010	0.0112	0.0002	731	46	371	7	308	6
22	0.42	11.3867	0.2971	0.4845	0.0099	0.1297	0.0025	2547	34	2555	24	2547	43
23	1.67	1.1099	0.0294	0.1057	0.0022	0.0344	0.0007	1044	45	758	14	648	13
24	0.92	0.3049	0.0124	0.0302	0.0007	0.0111	0.0003	1603	65	270	10	192	4
25	0.42	1.2492	0.0277	0.1316	0.0027	0.0415	0.0008	881	42	823	12	797	15
26	0.32	1.4363	0.0317	0.1344	0.0027	0.0365	0.0007	1065	41	904	13	813	16

27	0.42	6.4255	0.1443	0.3639	0.0074	0.1040	0.0019	2068	35	2036	20	2001	35
28	0.45	11.5205	0.2531	0.4813	0.0098	0.1286	0.0024	2579	33	2566	21	2533	43
29	0.90	1.3614	0.0311	0.1287	0.0026	0.0450	0.0008	1078	41	873	13	781	15
30	0.57	1.1622	0.0261	0.1230	0.0025	0.0380	0.0007	848	43	783	12	748	14
31	0.60	9.9234	0.2974	0.4552	0.0094	0.1149	0.0022	2467	35	2428	28	2418	42
32	0.84	1.2302	0.0335	0.1324	0.0027	0.0400	0.0008	838	46	814	15	802	16
33	1.03	1.3582	0.0313	0.1313	0.0027	0.0426	0.0008	1047	42	871	13	796	15
34	0.94	0.3893	0.0121	0.0447	0.0009	0.0143	0.0003	666	57	334	9	282	6
35	1.16	1.0995	0.0267	0.1131	0.0023	0.0355	0.0007	891	44	753	13	691	13
36	0.68	2.0738	0.0493	0.1937	0.0040	0.0570	0.0011	1077	41	1140	16	1141	21
37	0.62	0.4660	0.0106	0.0609	0.0013	0.0189	0.0004	422	47	388	7	381	8
38	1.30	1.3676	0.0339	0.1326	0.0027	0.0327	0.0006	1059	43	875	15	803	16
39	1.14	2.5284	0.1310	0.2250	0.0049	0.0731	0.0016	1376	54	1280	38	1308	26
40	0.16	1.8218	0.0410	0.1767	0.0036	0.0529	0.0010	1096	41	1053	15	1049	20
41	0.20	10.6568	0.2444	0.4672	0.0096	0.1299	0.0025	2493	34	2494	21	2471	42
42	0.57	1.4134	0.0316	0.1339	0.0027	0.0450	0.0008	1079	41	895	13	810	16
43	0.88	3.8194	0.0872	0.2777	0.0057	0.0812	0.0015	1591	38	1597	18	1580	29
44	0.67	1.1688	0.0289	0.1137	0.0023	0.0357	0.0007	1015	43	786	14	694	14
45	0.70	1.1406	0.0329	0.1179	0.0024	0.0400	0.0008	1048	46	773	16	718	14
46	0.47	0.5489	0.0125	0.0655	0.0014	0.0218	0.0004	627	45	444	8	409	8
47	0.48	0.5531	0.0118	0.0513	0.0011	0.0151	0.0003	1138	40	447	8	322	6
48	1.00	1.1931	0.0296	0.1257	0.0026	0.0400	0.0008	842	44	797	14	763	15

49	0.61	1.2029	0.0301	0.1190	0.0025	0.0405	0.0008	1032	43	802	14	725	14
50	0.92	0.3084	0.0128	0.0429	0.0009	0.0142	0.0003	300	79	273	10	271	6
51	0.65	0.2565	0.0059	0.0334	0.0007	0.0110	0.0002	413	48	232	5	212	4
52	0.36	1.5835	0.0380	0.1499	0.0031	0.0486	0.0009	1076	42	964	15	900	17
53	0.69	5.0186	0.1256	0.3252	0.0067	0.0923	0.0017	1775	37	1823	21	1815	33
54	0.62	0.6104	0.0154	0.0727	0.0015	0.0251	0.0005	639	48	484	10	452	9
55	0.58	0.6367	0.0194	0.0431	0.0009	0.0226	0.0005	1775	46	500	12	272	6
56	0.42	0.5051	0.0110	0.0564	0.0012	0.0205	0.0004	763	43	415	7	354	7
57	0.97	1.2728	0.0338	0.1328	0.0027	0.0393	0.0008	865	45	834	15	804	16
58	0.82	10.5311	0.2373	0.4631	0.0095	0.1303	0.0024	2505	34	2483	21	2453	42
59	1.32	0.5405	0.0130	0.0606	0.0013	0.0202	0.0004	749	46	439	9	379	8
60	0.68	1.5992	0.0370	0.1507	0.0031	0.0463	0.0009	1089	41	970	14	905	17
61	0.75	1.6694	0.0416	0.1543	0.0032	0.0423	0.0008	1162	42	997	16	925	18
62	0.51	0.5849	0.0126	0.0683	0.0014	0.0224	0.0004	654	44	468	8	426	8
63	0.15	0.6009	0.0133	0.0755	0.0016	0.0239	0.0005	479	46	478	8	469	9
64	0.86	1.3408	0.0323	0.1406	0.0029	0.0443	0.0008	906	43	864	14	848	16
65	0.93	1.1427	0.0304	0.1246	0.0026	0.0385	0.0007	845	46	774	14	757	15
66	0.23	0.3618	0.0158	0.0436	0.0010	0.0173	0.0005	579	77	314	12	275	6
67	0.97	1.2208	0.0312	0.1337	0.0028	0.0432	0.0008	847	45	810	14	809	16
68	0.64	1.2318	0.0333	0.1296	0.0027	0.0431	0.0008	853	46	815	15	785	15
69	0.21	13.2563	0.3116	0.5174	0.0107	0.0857	0.0017	2719	33	2698	22	2688	45
70	1.01	10.9151	0.2355	0.4724	0.0097	0.1176	0.0022	2522	34	2516	20	2494	43

71	0.34	0.3282	0.0091	0.0381	0.0008	0.0146	0.0003	672	53	288	7	241	5
72	0.75	1.2521	0.0309	0.1243	0.0026	0.0393	0.0008	1018	43	824	14	755	15
73	0.58	1.3772	0.0309	0.1344	0.0028	0.0474	0.0009	1062	41	879	13	813	16
74	0.51	1.3155	0.1737	0.1408	0.0046	0.0731	0.0049	1696	133	853	76	849	26
75	0.45	4.5844	0.1570	0.3073	0.0064	0.0817	0.0016	1707	40	1746	29	1727	32
76	1.41	0.7824	0.0179	0.0878	0.0018	0.0251	0.0005	752	44	587	10	543	11
77	0.68	0.7352	0.0163	0.0821	0.0017	0.0256	0.0005	792	43	560	10	509	10
78	0.32	1.7627	0.0394	0.1676	0.0035	0.0525	0.0010	1060	41	1032	14	999	19
79	0.51	1.7034	0.0390	0.1614	0.0033	0.0495	0.0009	1105	41	1010	15	965	18
80	0.70	0.5408	0.0122	0.0662	0.0014	0.0216	0.0004	625	45	439	8	413	8
81	0.37	6.5400	0.1515	0.3493	0.0072	0.0671	0.0013	2178	35	2051	20	1931	34
82	0.69	1.3428	0.0327	0.1404	0.0029	0.0446	0.0009	909	43	865	14	847	16
83	0.41	7.2293	0.1620	0.3901	0.0081	0.1104	0.0021	2147	35	2140	20	2124	37
84	0.46	0.5256	0.0120	0.0496	0.0010	0.0252	0.0005	1169	42	429	8	312	6
85	0.86	1.1415	0.0295	0.1223	0.0025	0.0374	0.0007	829	45	773	14	744	15
86	0.53	1.2110	0.0263	0.1246	0.0026	0.0370	0.0007	939	41	806	12	757	15
87	0.54	1.1971	0.0279	0.1172	0.0024	0.0370	0.0007	1031	42	799	13	714	14
88	0.97	3.3829	0.2081	0.2533	0.0056	0.0716	0.0017	1573	55	1500	48	1455	29
89	0.30	5.1252	0.1164	0.3251	0.0067	0.0935	0.0018	1853	36	1840	19	1815	33
90	0.20	20.1534	0.4321	0.5286	0.0109	0.1446	0.0027	3333	31	3099	21	2736	46
91	0.43	1.7680	0.0432	0.1587	0.0033	0.0512	0.0010	1178	41	1034	16	949	18
92	0.91	1.3671	0.0372	0.1284	0.0027	0.0378	0.0007	1100	44	875	16	779	15

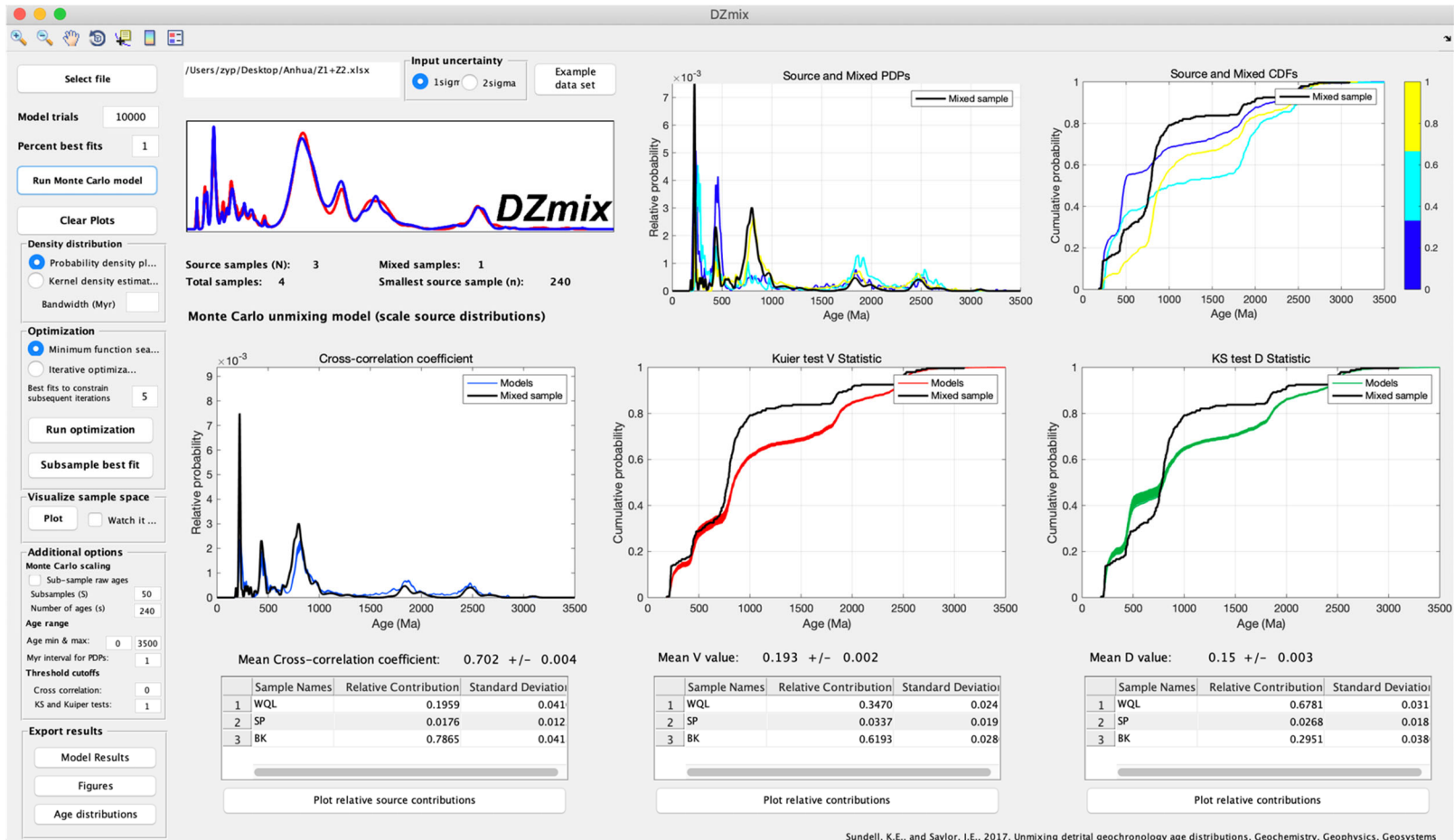
93	1.04	1.2435	0.0346	0.1321	0.0028	0.0394	0.0008	855	46	821	16	800	16
94	0.64	1.0650	0.0350	0.1278	0.0027	0.0445	0.0009	971	51	736	17	775	15
95	0.98	0.4592	0.0118	0.0450	0.0009	0.0147	0.0003	1047	46	384	8	284	6
96	0.56	1.6572	0.0360	0.1607	0.0033	0.0474	0.0009	1045	41	992	14	961	18
97	0.66	0.3469	0.0086	0.0465	0.0010	0.0143	0.0003	319	51	302	6	293	6
98	0.96	0.9326	0.0207	0.0983	0.0020	0.0306	0.0006	892	42	669	11	605	12
99	1.06	1.1193	0.0352	0.1199	0.0025	0.0389	0.0008	860	50	763	17	730	15
100	0.23	1.6336	0.0430	0.1500	0.0031	0.0388	0.0008	1178	42	983	17	901	18
101	0.29	5.2612	0.1267	0.3218	0.0067	0.0873	0.0017	1932	36	1863	21	1799	33
102	0.60	1.8631	0.0703	0.1776	0.0038	0.0546	0.0013	2161	44	1068	25	1054	21
103	0.44	6.1372	0.1404	0.3609	0.0075	0.0681	0.0013	2011	36	1996	20	1986	35
104	0.50	0.5546	0.0141	0.0595	0.0012	0.0183	0.0004	898	46	448	9	372	8
105	1.16	1.2421	0.0320	0.1325	0.0028	0.0411	0.0008	863	45	820	14	802	16
106	0.53	1.8030	0.0454	0.1781	0.0037	0.0543	0.0010	1009	43	1047	16	1056	20
107	0.18	5.1940	0.1265	0.3284	0.0068	0.0886	0.0017	1874	37	1852	21	1831	33
108	0.10	7.6392	0.2018	0.4043	0.0084	0.0978	0.0020	2189	35	2190	24	2189	39
109	0.82	1.2474	0.0287	0.1333	0.0028	0.0347	0.0007	963	42	822	13	807	16
110	1.20	0.6471	0.0151	0.0792	0.0016	0.0243	0.0005	606	46	507	9	491	10
111	0.99	1.0207	0.0345	0.1176	0.0025	0.0378	0.0008	735	54	714	17	717	14
112	0.56	1.0006	0.0247	0.0958	0.0020	0.0362	0.0007	1082	43	704	13	590	12
113	1.05	1.0124	0.0224	0.1158	0.0024	0.0344	0.0006	732	43	710	11	706	14
114	1.11	0.8734	0.0202	0.1032	0.0021	0.0344	0.0007	680	45	637	11	633	13

115	0.40	0.4612	0.0118	0.0608	0.0013	0.0189	0.0004	381	51	385	8	380	8
116	0.86	1.1219	0.0322	0.1237	0.0026	0.0401	0.0008	790	48	764	15	752	15
117	0.36	9.9896	0.3320	0.4508	0.0095	0.1186	0.0023	2486	35	2434	31	2399	42
118	0.45	4.9938	0.1296	0.3156	0.0066	0.1000	0.0019	1811	37	1818	22	1768	32
119	0.51	1.4604	0.0326	0.1429	0.0030	0.0469	0.0009	1024	41	914	13	861	17
120	0.96	1.0762	0.0329	0.1124	0.0024	0.0377	0.0007	918	49	742	16	687	14
121	1.52	1.1510	0.0334	0.1160	0.0024	0.0378	0.0007	912	47	778	16	707	14

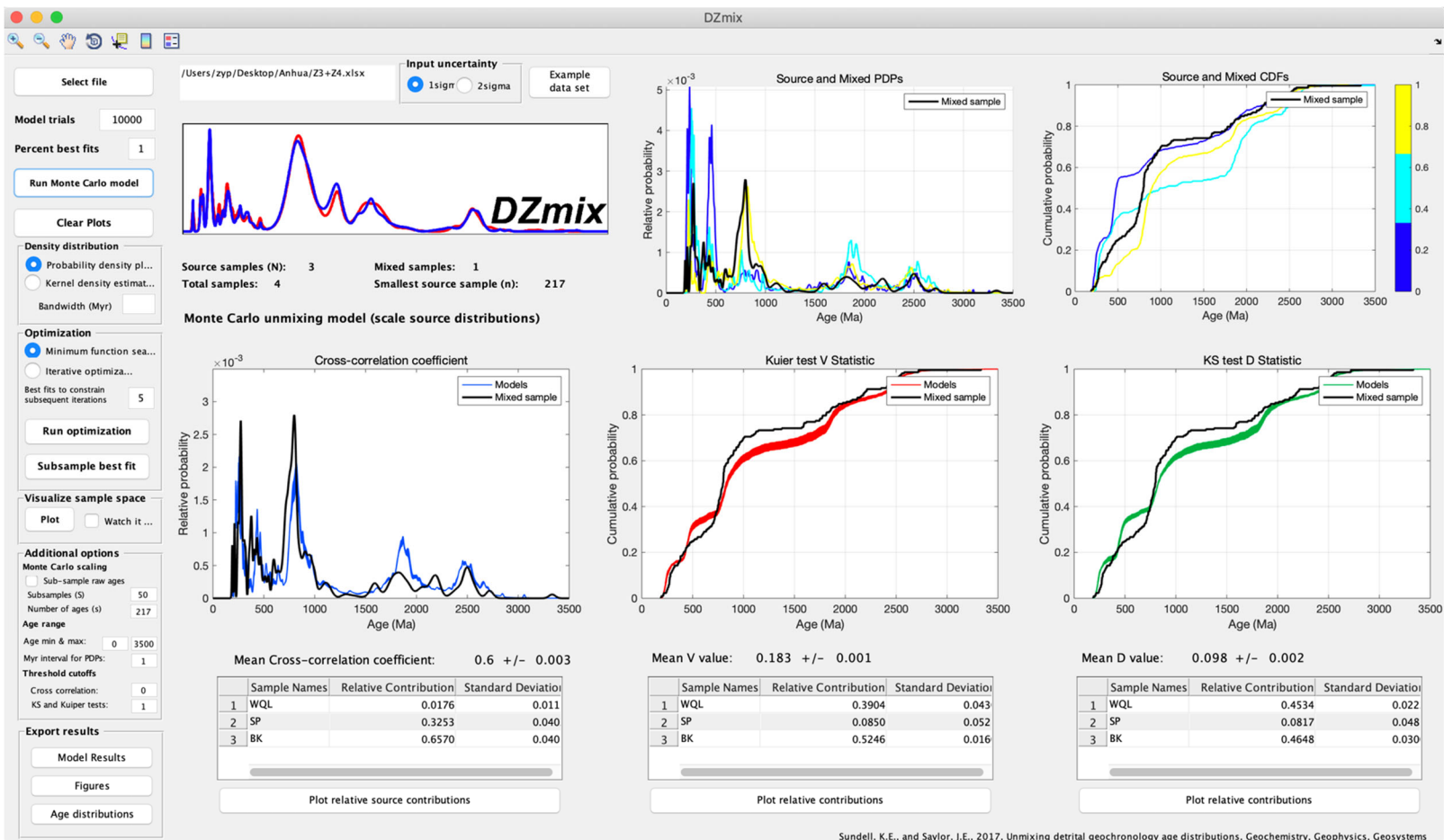
Table S4. Quantitative comparison of age distributions for the Anhua basin (Z1&Z2; Z3&Z4).

	cross correlation coefficient	mean cross correlation	0.702 ± 0.004	Kupier test	mean V value	0.193 ± 0.002	K-S test	mean D value	0.15 ± 0.003
Z1+Z2	sample	relative contribution	standard deviation	sample	relative contribution	standard deviation	sample	relative contribution	standard deviation
	WQL	0.1959	0.041	WQL	0.3470	0.024	WQL	0.6781	0.031
	SP	0.0176	0.012	SP	0.0337	0.019	SP	0.0268	0.018
	BK	0.7865	0.041	BK	0.6193	0.028	BK	0.2951	0.038
Z3+Z4	cross correlation coefficient	mean cross correlation	0.6 ± 0.003	Kupier test	mean V value	0.183 ± 0.001	K-S test	mean D value	0.098 ± 0.002
	sample	relative contribution	standard deviation	sample	relative contribution	standard deviation	sample	relative contribution	standard deviation
	WQL	0.0176	0.011	WQL	0.3904	0.043	WQL	0.4534	0.022
	SP	0.3253	0.040	SP	0.0850	0.052	SP	0.0817	0.048
	BK	0.6570	0.040	BK	0.5246	0.016	BK	0.4648	0.030
Monte Carlo simulation: 10,000; Percent best fits: 1%									
WQL- West Qinling belt; SG- Songpan-Ganzi terrane; BK- Bikou terrane & northern Sichuan basin.									

a) DZmix main screen following Monte Carlo calculation of relative contributions for “Z1+Z2”.



b) DZmix main screen following Monte Carlo calculation of relative contributions for “Z3+Z4”.



Any use of trade, firm, or product names is for descriptive purposes only and does not imply endorsement by the U.S. Government.

Andersen, T. (2002). Correction of common lead in U-Pb analyses that do not report 204 Pb. *Chemical Geology*, 192(1–2), 59–79. [https://doi.org/10.1016/S0009-2447\(01\)00432-7](https://doi.org/10.1016/S0009-2447(01)00432-7)

[2541\(02\)00195-X](#)

- Cañón-Tapia, E. (1994). Anisotropy of magnetic susceptibility parameters: Guidelines for their rational selection. *Pure and Applied Geophysics*, 142(2), 365–382.
<https://doi.org/10.1007/BF00879310>
- DeCelles, P. G., Gray, M. B., Ridgway, K. D., Cole, R. B., Pivnik, D. A., Pequera, N., & Srivastava, P. (1991). Controls on synorogenic alluvial-fan architecture, Beartooth Conglomerate (Palaeocene), Wyoming and Montana. *Sedimentology*, 38(4), 567-590. <http://dx.doi.org/10.1111/j.1365-3091.1991.tb01009.x>
- Ellwood, B. B. (1978). Flow and emplacement direction determined for selected basaltic bodies using magnetic susceptibility anisotropy measurements. *Earth and Planetary Science Letters*, 41(3), 254-264. <http://www.sciencedirect.com/science/article/pii/0012821X78901826>
- Fang, X. M., Garzione, C., Van der Voo, R., Li, J. J., & Fan, M. J. (2003). Flexural subsidence by 29 Ma on the NE edge of Tibet from the magnetostratigraphy of Linxia Basin, China. *Earth and Planetary Science Letters*, 210(3–4), 545-560. <http://www.sciencedirect.com/science/article/pii/S0012821X03001420>
- Fisher, R. (1953). Dispersion on a Sphere. *Royal Society of London*, 217(1130), 295-305.
- Fossen, H. (2010). *Structural Geology*. New York: Cambridge University Press.
- GBGMR, G. B. o. G. a. M. R. (1971). Geologic Map of the Lintan Region, with Regional Geologic Report (1:20,000 Scale).
- Gehrels, G., Valencia, V., & Pullen, A. (2006). Detrital zircon geochronology by laser-ablation multicollector ICPMS at the Arizona LaserChron Center. *The Paleontological Society Papers*, 12, 67-76. <https://doi.org/10.1017/S1089332600001352>
- Jones, C. H. (2002). User-driven integrated software lives: “Paleomag” paleomagnetics analysis on the Macintosh. *Computers & geosciences*, 28(10), 1145–1151.
[https://doi.org/10.1016/S0098-3004\(02\)00032-8](https://doi.org/10.1016/S0098-3004(02)00032-8)
- Kent, D. V., & Lowrie, W. (1975). On the magnetic susceptibility anisotropy of deep-sea sediment. *Earth and Planetary Science Letters*, 28(1), 1-12.
<http://www.sciencedirect.com/science/article/pii/0012821X75900679>
- Li, C., Qiu, Z., & Downs, W. (1980). Early Miocene mammalian fossils of the Xining Basin, Qinghai Province. *Vertebrata Palasiatica*, 18(3), 198-209.
- Liu, Y., Hu, Z., Gao, S., Günther, D., Xu, J., Gao, C., & Chen, H. (2008). In situ analysis of major and trace elements of anhydrous minerals by LA-ICP-MS without applying an internal standard. *Chemical Geology*, 257(1-2), 34-43. <https://doi.org/10.1016/j.chemgeo.2008.08.004>
- Mcfadden, P. L., & Mcelhinny, M. W. (1990). Classification of the reversal test in palaeomagnetism. *Geophysical Journal International*, 103(3), 725-729.
- Miall, A. D. (1978). *Principles of sedimentary basin analysis*. New York: Springer Science.
- QBGMR, Q. B. o. G. a. M. R. (1971). Geologic Map of the Zeku Region, with Regional Geologic Report (1:20,000 Scale).
- Qiu, Z., Xie, J., & Yan, D. (1990). Discovery of some Early Miocene mammalian fossils from Dongxiang, Gansu. *Palasiatica*, 28, P-24.

- Wang, S. Q., Liu, S. P., Xie, G. P., Liu, J., Peng, T. J., Hou, S. K., & Palasiatica, V. (2013). *Gomphotherium wimani* from Wushan County, China, and its implications for the Miocene stratigraphy of the Tianshui area. *Vertebrata Palasiatica*, 51(1), 71-84.
- Wang, Z., Zhang, P., Garzione, C. N., Lease, R. O., Zhang, G., Zheng, D., et al. (2012). Magnetostratigraphy and depositional history of the Miocene Wushan basin on the NE Tibetan plateau, China: Implications for middle Miocene tectonics of the West Qinling fault zone. *Journal of Asian Earth Sciences*, 44(1), 189–202.
<https://doi.org/10.1016/j.jseaes.2011.06.009>
- Zhang, Y., & Xue, X. (1994). *Taphonomy of Longjiagou Hipparrionine Fauna (Turolian, Miocene) Wudu County, Gansu Province, China*. Beijing: Geological Publishing House.